



Trends in
**Applied Sciences
Research**

ISSN 1819-3579



Academic
Journals Inc.

www.academicjournals.com

Electrochemical Properties of Cathode $\text{LiNi}_{1-y}\text{Ti}_y\text{O}_2$ Synthesized by Milling and Solid-State Reaction Method

¹MyoungYoup Song, ¹ChanGi Park, ²SunDo Youn, ²YoungHo Na and ²HyeRyoung Park

¹Division of Advanced Materials Engineering, Research Center of Advanced Materials Development, Engineering Research Institute, Chonbuk National University, 664-14 Iga Deogjindong Deogjingu Jeonju, 561-756, Republic of Korea

²Division of Applied Chemical Engineering, Chonnam National University, 300 Yongbongdong Bukgu Gwangju, 500-757, Republic of Korea

Abstract: $\text{LiNi}_{1-y}\text{Ti}_y\text{O}_2$ ($y = 0.005, 0.01, 0.025, 0.05$ and 0.1) were synthesized by milling and solid-state method. Their electrochemical properties were then compared with those of $\text{LiNi}_{1-y}\text{M}_y\text{O}_2$ ($M = \text{Ga}^{3+}$ and In^{3+}). All the samples had the $\text{R}\bar{3}\text{m}$ structure. $\text{LiNi}_{0.95}\text{Ti}_{0.05}\text{O}_2$ has the largest first discharge capacity 179.8 mAh g^{-1} and the discharge capacity 113.8 mAh g^{-1} at the 20th cycle. $\text{LiNi}_{0.995}\text{Ti}_{0.005}\text{O}_2$ has the smallest first discharge capacity 125.4 mAh g^{-1} . The samples exhibit similar cycling performances. $\text{LiNi}_{0.975}\text{Ga}_{0.025}\text{O}_2$ and $\text{LiNi}_{0.9}\text{In}_{0.1}\text{O}_2$ had the best electrochemical properties among the samples substituted by the same element, respectively. Among $\text{LiNi}_{0.975}\text{Ga}_{0.025}\text{O}_2$, $\text{LiNi}_{0.9}\text{In}_{0.1}\text{O}_2$ and $\text{LiNi}_{0.95}\text{Ti}_{0.05}\text{O}_2$, $\text{LiNi}_{0.95}\text{Ti}_{0.05}\text{O}_2$ has the largest first discharge capacity, but has the worst cycling performance. $\text{LiNi}_{0.975}\text{Ga}_{0.025}\text{O}_2$ has the smallest first discharge capacity, but has the smallest capacity degradation rate $0.70 \text{ mAh g}^{-1} \text{ cycle}^{-1}$.

Key words: $\text{LiNi}_{1-y}\text{Ti}_y\text{O}_2$, milling, solid-state reaction method, electrochemical properties, $I_{0.07}/I_{1.04}$, R-factor

Introduction

The transition metal oxides such as LiMn_2O_4 (Tarascon *et al.*, 1991; Armstrong and Bruce, 1996; Song and Ahn, 1998), LiCoO_2 (Ozawa, 1994; Alcatara *et al.*, 1997; Peng *et al.*, 1998) and LiNiO_2 (Dahn *et al.*, 1990, 1991; Marini *et al.*, 1991; Ebner *et al.*, 1994) have been investigated in order to apply them to the cathode materials of lithium secondary battery. LiMn_2O_4 is very cheap and does not bring about environmental pollution, but its cycling performance is not good. LiCoO_2 has a large diffusivity and a high operating voltage and it can be easily prepared. However, it has a disadvantage that it contains an expensive element Co. LiNiO_2 is a very promising cathode material since it has a large discharge capacity (Nishida *et al.*, 1997) and is relatively excellent from the view points of economics and environment. On the other hand, its preparation is very difficult as compared with LiCoO_2 and LiMn_2O_4 .

It is known that $\text{Li}_{1-x}\text{Ni}_{1+x}\text{O}_2$ forms rather than stoichiometric LiNiO_2 during preparation. This phenomenon is called cation mixing. Excess nickel occupies the Li sites, destroying the ideally layered structure and preventing lithium ions from easy movement for intercalation and deintercalation during cycling. This results in a small discharge capacity and a poor cycling performance. To solve the problem of cation mixing, Co^{3+} , Al^{3+} , Mn^{3+} and Ti^{4+} ions were substituted for lithium ion in LiNiO_2

Corresponding Author: MyoungYoup Song, Division of Advanced Materials Engineering, Research Center of Advanced Materials Development, Engineering Research Institute, Chonbuk National University, 664-14 Iga Deogjindong Deogjingu Jeonju, 561-756, Republic of Korea Tel: +82-63-270-2379 Fax: +82-63-270-2386

(Gao *et al.*, 1998; Kim and Amine, 2001; Broussely, 1999; Caurant *et al.*, 1996; Zhang *et al.*, 2004; Amriou *et al.*, 2004; Shinova *et al.*, 2005). According to Kim and Amine (2001, 2002) and Gao *et al.* (1998), the substitution of Ti for Ni resulted in a large discharge capacity and a good cycling performance.

In this study $\text{LiNi}_{1-y}\text{Ti}_y\text{O}_2$ ($y = 0.005, 0.01, 0.025, 0.05$ and 0.1) were synthesized by milling and solid-state method and the electrochemical properties of the synthesized samples were investigated. Their electrochemical properties were then compared with those of $\text{LiNi}_{1-y}\text{M}_y\text{O}_2$ ($M = \text{Ga}^{3+}$ and In^{3+}) synthesized by the same method in our earlier study (Kim *et al.*, 2005a,b). The substituted Ga and In have the same oxidation number as Ti.

Materials and Methods

The $\text{LiNi}_{1-y}\text{Ti}_y\text{O}_2$ ($y = 0.005, 0.01, 0.025, 0.05$ and 0.1) are synthesized by milling and solid-state method under the optimum conditions for the preparation of LiNiO_2 , previously studied (Kim *et al.*, 2005). $\text{LiOH} \cdot \text{H}_2\text{O}$ (Kojundo Chemical Lab. Co., Ltd, purity 99%), $\text{Ni}(\text{OH})_2$ (Kojundo Chemical Lab. Co., Ltd, purity 99.9%), TiNO_3 (Aldrich Chemical, 99.9%) are used as starting materials. The starting materials are mechanically mixed by SPEX milling for 1 h. The mixed materials are preheated at 450°C for 5 h in air, then pressed into pellet and calcined at 750°C for 30 h under oxygen stream. The phase identification of the synthesized samples is carried out by X-ray powder diffraction analysis (Rigaku III/A diffractometer) using $\text{Cu K}\alpha$ radiation. The scanning rate is 6°min^{-1} and the scanning range of diffraction angle (2θ) is $10^\circ \leq 2\theta \leq 80^\circ$. The electrochemical cells consist of $\text{LiNi}_{1-y}\text{Ti}_y\text{O}_2$ as a positive electrode, Li foil as a negative electrode and electrolyte [Purelyte (Samsung General Chemicals Co., Ltd.)] prepared by solving 1M LiPF_6 in a 1:1 (volume ratio) mixture of Ethylene Carbonate (EC) and diethyl carbonate (DEC). The positive electrode consists of 85 wt.% synthesized materials, 10 wt.%

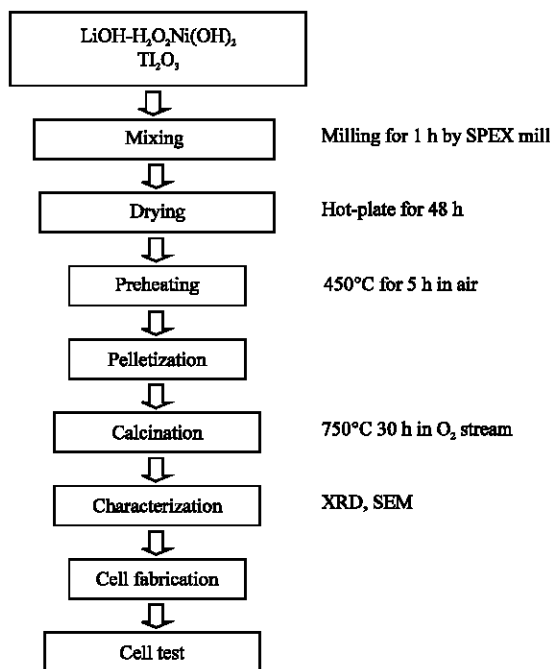


Fig. 1: Experimental procedure for $\text{LiNi}_{1-y}\text{Ti}_y\text{O}_2$ electrode prepared by solid-state reaction method after milling

acetylene black and 5 wt.% polyvinylidene fluoride (PVDF) binder solved in 1-Methyl-2-pyrrolidinone (NMP). A Whatman glass-fiber is used as a separator. The cells are assembled in argon-filled dry box and the cell type is coin-type (2016). All the electrochemical tests are performed at room temperature with a potentiostatic/galvanostatic system. The cells are cycled between 2.7 and 4.2 V at 0.1 C-rate.

Figure 1 shows experimental procedure for the $\text{LiNi}_{1-y}\text{Tl}_y\text{O}_2$ electrodes prepared by milling and solid-state reaction method.

Results and Discussion

Figure 2 shows X-ray powder diffraction (XRD) patterns of $\text{LiNi}_{1-y}\text{Tl}_y\text{O}_2$ ($y = 0.005, 0.01, 0.025, 0.05$ and 0.1) calcined at 750°C for 30 h. All the samples have only the phase with $R\bar{3}m$ structure and do not exhibit the peaks of impurity. The $R\bar{3}m$ structure is distorted in c-axis direction. This is reflected by the split of 006 and 102 peaks and of 108 and 110 peaks in the XRD patterns. The 108 and 110 peaks were split for all the samples.

It is generally known that the cation mixing is small if the intensity ratio of 003 peak to 104 peak (I_{003}/I_{104}) is large (Ohzuku *et al.*, 1993). The value of $(I_{006}+I_{102})/I_{101}$, called R-factor, is known to be smaller when the hexagonal ordering is high (Dahn *et al.*, 1990). In addition, the split between 108 and 110 peaks is reported to suggest the smaller cation mixing and the better hexagonal ordering (Ohzuku *et al.*, 1993).

Table 1 gives the lattice parameters a , c , c/a , I_{003}/I_{104} , R-factor and unit cell volume calculated from XRD patterns of $\text{LiNi}_{1-y}\text{Tl}_y\text{O}_2$ ($y = 0.005, 0.01, 0.025, 0.05$ and 0.1) calcined at 750°C for 30 h. The sample with $y = 0.005$ has the largest I_{003}/I_{104} and all the samples have the smallest value of R-factor.

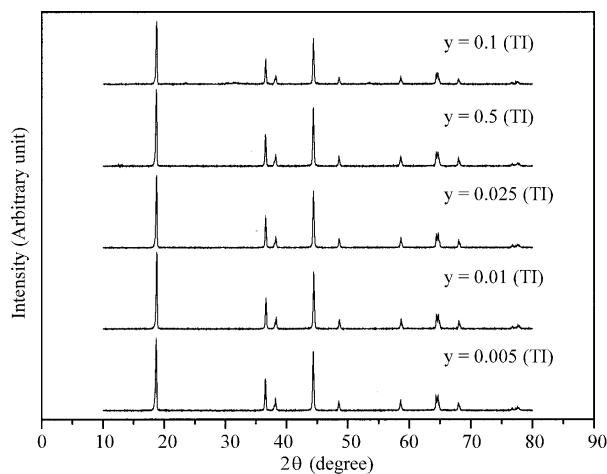


Fig. 2: XRD patterns of $\text{LiNi}_{1-y}\text{Tl}_y\text{O}_2$ ($y = 0.005, 0.01, 0.025, 0.05$ and 0.1) calcined at 750°C for 30 h

Table 1: Data calculated from XRD patterns of $\text{LiNi}_{1-y}\text{Tl}_y\text{O}_2$ ($y = 0.005, 0.01, 0.025, 0.05$ and 0.1) calcined at 750°C for 30 h

	$a(\text{\AA})$	$c(\text{\AA})$	I_{003}/I_{104}	R-factor	Unit cell volume (\AA^3)
$y = 0.1$	2.786	14.178	1.02	0.59	101.872
$y = 0.05$	2.880	14.223	1.12	0.53	101.320
$y = 0.025$	2.877	14.195	1.05	0.56	102.240
$y = 0.01$	2.877	14.207	0.98	0.52	101.843
$y = 0.005$	2.882	14.239	1.16	0.50	102.108

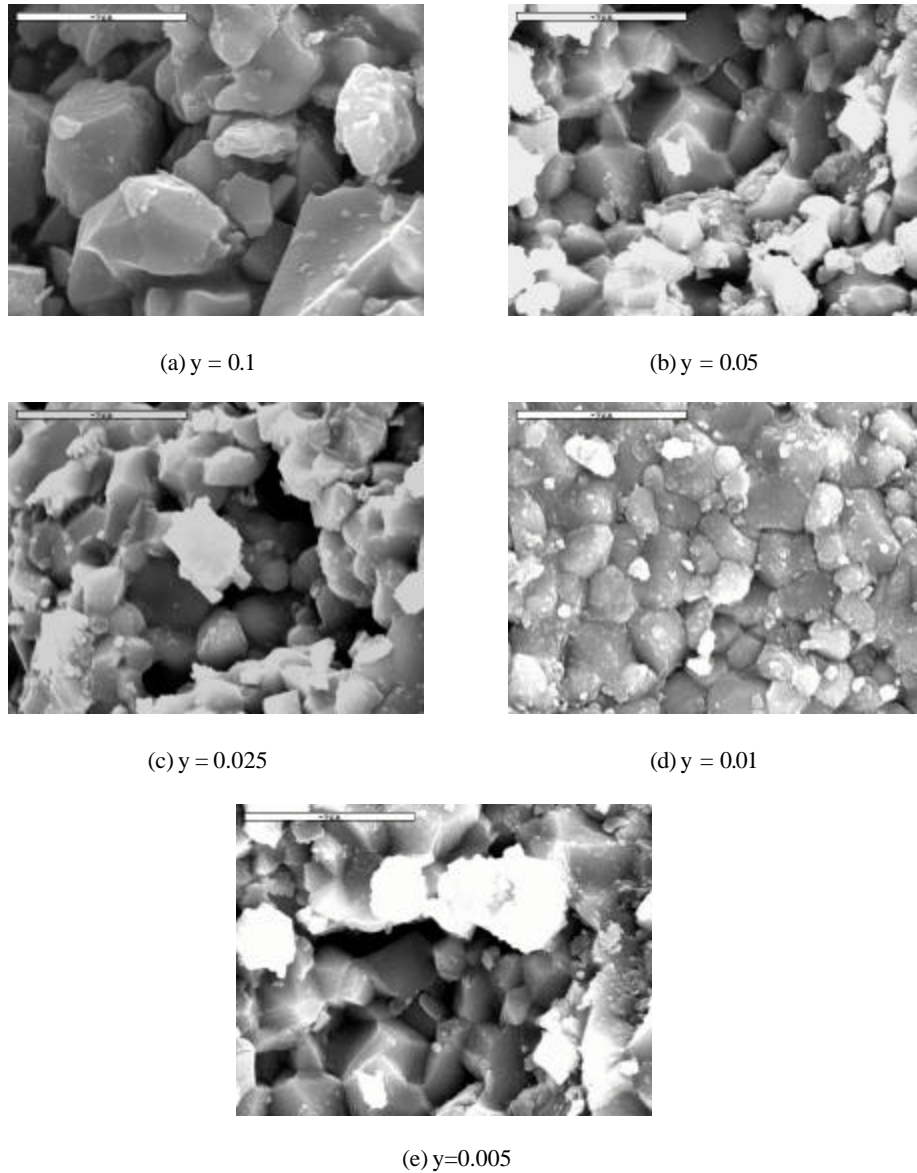


Fig. 3: SEM photographs of $\text{LiNi}_{1-y}\text{Ti}_y\text{O}_2$ ($y = 0.005, 0.01, 0.025, 0.05$ and 0.1) calcined at 750°C for 30 h

Figure 3 shows the SEM photographs of $\text{LiNi}_{1-y}\text{Ti}_y\text{O}_2$ ($y = 0.005, 0.01, 0.025, 0.05$ and 0.01) calcined at 750°C for 30 h. The samples contain small and large particles. The particles become larger as the value of y increases.

Figure 4 shows the variations of the discharge capacity of $\text{LiNi}_{1-y}\text{Ti}_y\text{O}_2$ ($y = 0.005, 0.01, 0.025, 0.05$ and 0.01) calcined at 750°C for 30 h. The sample with $y = 0.05$ has the largest first discharge capacity 179.8 mAh g^{-1} and the discharge capacity 113.8 mAh g^{-1} at the 20th cycle. The sample with $y = 0.005$ has the smallest first discharge capacity 125.4 mAh g^{-1} . The samples exhibit similar cycling performance.

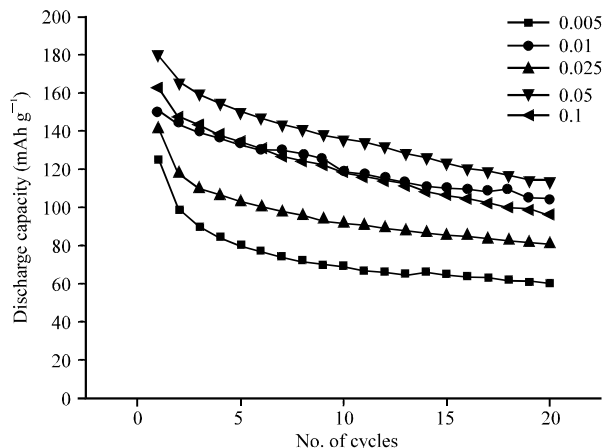


Fig. 4: Variations of discharge capacity at 0.1C-rate with the number of cycles for $\text{LiNi}_{1-y}\text{Tl}_y\text{O}_2$ ($y = 0.005, 0.01, 0.025, 0.05$ and 0.1) calcined at 750°C for 30 h

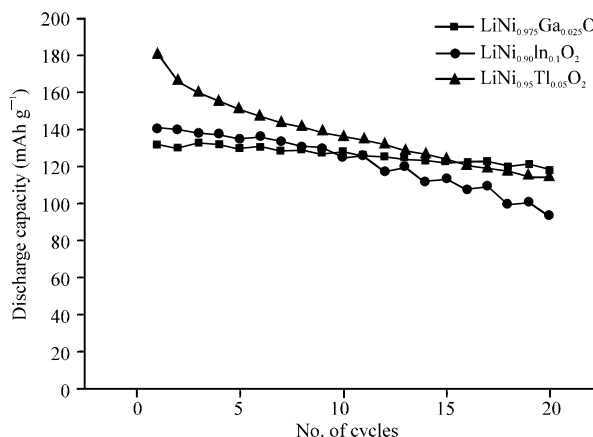


Fig. 5: Variations of discharge capacity at 0.1 C-rate with the number of cycles for $\text{LiNi}_{1-y}\text{M}_y\text{O}_2$ ($M = \text{Ga}, y = 0.025; M = \text{In}, y = 0.1; M = \text{Tl}, y = 0.05$) calcined at 750°C for 30 h

Table 2: Data calculated from X-ray powder diffraction patterns of $\text{LiNi}_{1-y}\text{M}_y\text{O}_2$ ($M = \text{Ga}, y = 0.025; M = \text{In}, y = 0.1; M = \text{Tl}, y = 0.05$) calcined at 750°C for 30 h

	a(Å)	c(Å)	I_{003}/I_{104}	R-factor	Unit cell volume (Å ³)
$\text{LiNi}_{0.975}\text{Ga}_{0.025}\text{O}_2$	2.883	14.362	0.92	0.54	103.380
$\text{LiNi}_{0.90}\text{In}_{0.1}\text{O}_2$	2.877	14.212	1.33	0.52	101.559
$\text{LiNi}_{0.95}\text{Tl}_{0.05}\text{O}_2$	2.880	14.223	1.12	0.53	101.320

In our earlier study (Kim *et al.*, 2005a, b), we studied the electrochemical properties of $\text{LiNi}_{1-y}\text{Ga}_y\text{O}_2$ and $\text{LiNi}_{1-y}\text{In}_y\text{O}_2$ synthesized by the same method, as mentioned above. Among $\text{LiNi}_{1-y}\text{Ga}_y\text{O}_2$ $\text{LiNi}_{0.975}\text{Ga}_{0.025}\text{O}_2$ had the best electrochemical properties. $\text{LiNi}_{0.9}\text{In}_{0.1}\text{O}_2$ exhibited the best electrochemical properties among $\text{LiNi}_{1-y}\text{In}_y\text{O}_2$.

Figure 5 shows the variations of the discharge capacity of $\text{LiNi}_{1-y}\text{M}_y\text{O}_2$ ($M = \text{Ga}, y = 0.025; M = \text{In}, y = 0.1; M = \text{Tl}, y = 0.05$) calcined at 750° for 30 h. The sample $\text{LiNi}_{0.95}\text{Tl}_{0.05}\text{O}_2$ has the largest first discharge capacity 179.8 mAh g^{-1} and the discharge capacity 113.8 mAh g^{-1} at the 20th

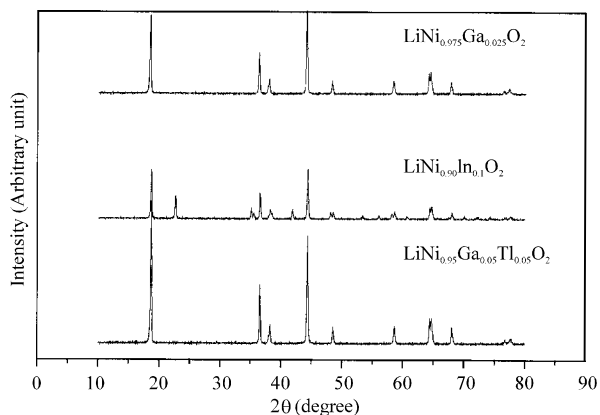


Fig. 6: X-ray powder diffraction patterns of $\text{LiNi}_{1-y}\text{M}_y\text{O}_2$ ($M = \text{Ga}, y = 0.025$; $M = \text{In}, y = 0.1$; $M = \text{Tl}, y = 0.05$) calcined at 750°C for 30 h

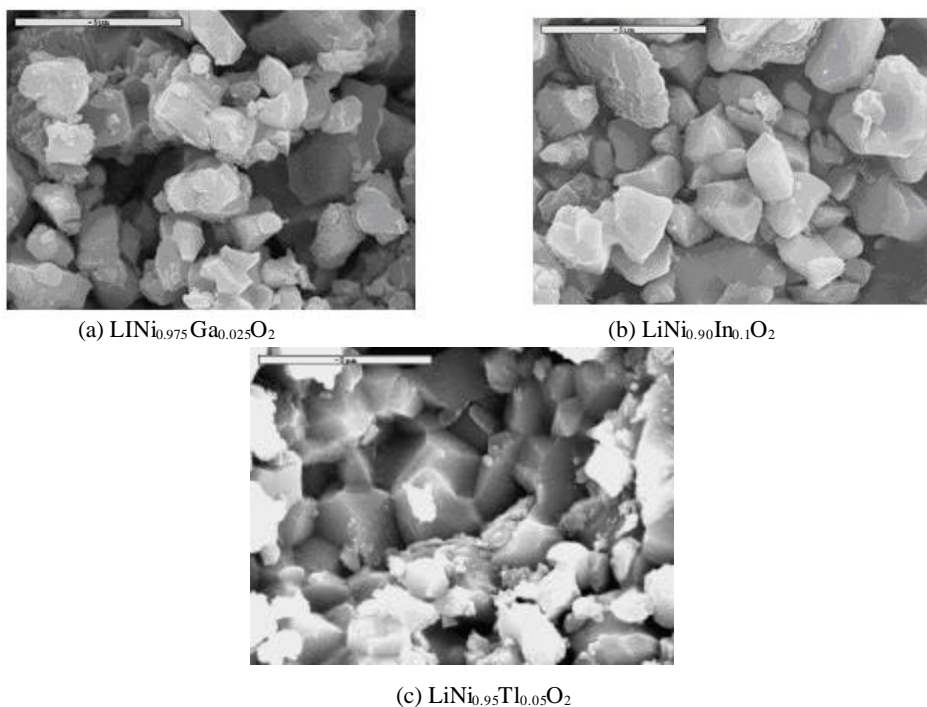


Fig. 7: SEM photographs of $\text{LiNi}_{1-y}\text{M}_y\text{O}_2$ ($M = \text{Ga}, y = 0.025$; $M = \text{In}, y = 0.1$; $M = \text{Tl}, y = 0.05$) calcined at 750°C for 30 h

cycle. The sample $\text{LiNi}_{0.975}\text{Ga}_{0.025}\text{O}_2$ has the smallest first discharge capacity 131.4 mAh g^{-1} , but it has the best cycling performance. $\text{LiNi}_{0.975}\text{Ga}_{0.025}\text{O}_2$ has the discharge capacity 117.5 mAh g^{-1} at the 20th cycle, showing the discharge capacity degradation rate of $0.70 \text{ mAh g}^{-1} \text{ cycle}^{-1}$.

Figure 6 shows XRD patterns of $\text{LiNi}_{0.975}\text{Ga}_{0.025}\text{O}_2$, $\text{LiNi}_{0.9}\text{In}_{0.1}\text{O}_2$ and $\text{LiNi}_{0.95}\text{Tl}_{0.05}\text{O}_2$. All the samples have the phase with $R\bar{3}m$ structure. In addition, $\text{LiNi}_{0.9}\text{In}_{0.1}\text{O}_2$ shows the peaks for LiInO_2 .

Table 2 gives the lattice parameters a, c, c/a, I_{003}/I_{104} , R-factor and unit cell volume calculated from XRD patterns of $\text{LiNi}_{1-y}\text{M}_y\text{O}_2$ (M = Ga, y = 0.025; M = In, y = 0.1; M = Tl, y = 0.05). $\text{LiNi}_{0.9}\text{In}_{0.1}\text{O}_2$ has the largest I_{003}/I_{104} and all the samples have the similar values of R-factor.

Figure 7 shows the SEM photographs of $\text{LiNi}_{0.975}\text{Ga}_{0.025}\text{O}_2$, $\text{LiNi}_{0.9}\text{In}_{0.1}\text{O}_2$ and $\text{LiNi}_{0.95}\text{Tl}_{0.05}\text{O}_2$ calcined at 750°C for 30 h. All the samples have small and large particle. The particle size increases roughly from $\text{LiNi}_{0.975}\text{Ga}_{0.025}\text{O}_2$ to $\text{LiNi}_{0.9}\text{In}_{0.1}\text{O}_2$ and then to $\text{LiNi}_{0.95}\text{Tl}_{0.05}\text{O}_2$. The particles of $\text{LiNi}_{0.95}\text{Tl}_{0.05}\text{O}_2$ are agglomerated.

Conclusions

$\text{LiNi}_{1-y}\text{Tl}_y\text{O}_2$ (y = 0.005, 0.01, 0.025, 0.05 and 0.1) were synthesized by milling for 1 h, preheating at 450°C for 5 h in air, then pelletizing and finally calcining at 750°C for 30 h under oxygen stream. All the samples had the $\bar{R}3m$ structure. $\text{LiNi}_{0.95}\text{Tl}_{0.05}\text{O}_2$ has the largest first discharge capacity 179.8 mAh g⁻¹ and the discharge capacity 113.8 mAh g⁻¹ at the 20th cycle. $\text{LiNi}_{0.995}\text{Tl}_{0.005}\text{O}_2$ has the smallest first discharge capacity 125.4 mAh g⁻¹. The samples exhibit similar cycling performances. $\text{LiNi}_{0.975}\text{Ga}_{0.025}\text{O}_2$ and $\text{LiNi}_{0.9}\text{In}_{0.1}\text{O}_2$ had the best electrochemical properties among the samples substituted by the same element, respectively. Among $\text{LiNi}_{0.975}\text{Ga}_{0.025}\text{O}_2$, $\text{LiNi}_{0.9}\text{In}_{0.1}\text{O}_2$ and $\text{LiNi}_{0.95}\text{Tl}_{0.05}\text{O}_2$, $\text{LiNi}_{0.95}\text{Tl}_{0.05}\text{O}_2$ has the largest first discharge capacity, but has the worst cycling performance. $\text{LiNi}_{0.975}\text{Ga}_{0.025}\text{O}_2$ has the smallest discharge capacity, but has the smallest capacity degradation rate 0.70 mAh g⁻¹ cycle⁻¹.

Acknowledgment

This study was supported by grant No. R01-2003-000-10325-0 from the Basic Research Program of the Korea Science and Engineering Foundation.

References

- Alcatara, R., P. Lavela, J.L. Tirado, R. Stoyanova and E. Zhecheva, 1997. Structure and electrochemical properties of boron-doped LiCoO_2 . *J. Solid State Chem.*, 134: 265-273.
- Amriou, T., A. Sayede, B. Khelifa, C. Mathieu and H. Aourag, 2004. Effect of Al-doping on lithium nickel oxides. *J. Power Sources*, 130: 213-220.
- Armstrong, A.R. and P.G. Bruce, 1996. Synthesis of layered LiMnO_2 as an electrode for rechargeable lithium batteries. *Lett. Nat.*, 381: 499-500.
- Broussely, M., 1999. Recent developments on lithium ion batteries at SAFT. *J. Power Sources*, 81-82: 140-143.
- Caurant, D., N. Baffier, B. Garcia, J.P. Pereira-Ramos, 1996. Synthesis by a soft chemistry route and characterization of $\text{LiNi}_x\text{Co}_{1-x}\text{O}_2$ (0 ≤ x ≤ 1) cathode materials. *Solid State Ionics*, 91: 45-54.
- Dahn, J.R., U. von Sacken and C.A. Michal, 1990. Structure and electrochemistry of $\text{Li}_{1+y}\text{NiO}_2$ and a new Li_2NiO_2 phase with the $\text{Ni}(\text{OH})_2$ structure. *Solid State Ion.*, 44: 87-97.
- Dahn, J.R., U. von Sacken, M.R. Jukow and H. Aljanaby, 1991. Rechargeable LiNiO_2 /varbon cells. *J. Electrochem. Soc.*, 138: 2207-2211.
- Ebner, W., D. Fouchard and L. Xie, 1994. The LiNiO_2 /carbon lithium-ion battery. *Solid State Ionics*, 69: 238-256.
- Gao, Y., M.V. Yakovleva and W.B. Ebner, 1998. Novel $\text{LiNi}_{1-x}\text{Ti}_{x/2}\text{Mg}_{x/2}\text{O}_2$ compounds as cathode materials for safer lithium-ion batteries. *Electrochem. Solid State Lett.*, 1: 117-119.
- Kim, J. and K. Amine, 2001. The effect of tetravalent titanium substitution in $\text{LiNi}_{1-x}\text{Ti}_x\text{O}_2$ (0.025 ≤ x ≤ 0.2) system. *Electrochem. Commun.*, 3: 52-55.

- Kim, J. and K. Amine, 2002. A comparative study on the substitution of divalent, trivalent and tetravalent metal ions in $\text{LiNi}_{1-x}\text{M}_x\text{O}_2$ ($\text{M} = \text{Cu}^{2+}$, Al^{3+} and Ti^{4+}). *J. Power Sources*, 104: 33-39.
- Kim, H.U., S.D. Youn, J.C. Lee, H.R. Park, C.G. Park and M.Y. Song, 2005a. Electrochemical properties of $\text{LiNi}_{1-y}\text{Ga}_y\text{O}_2$ synthesized by milling and solid-state reaction method. *J. Kor. Cer. Soc.*, 42: 631-636.
- Kim, H.U., S.D. Youn, J.C. Lee, H.R. Park, C.G. Park and M.Y. Song, 2005b. Electrochemical properties of $\text{LiNi}_{1-y}\text{In}_y\text{O}_2$ synthesized by milling and solid-state reaction method. *Trans. Kor. Hydrogen and New Energy Soc.*, 16: 385-392.
- Marini, A., V. Massarotti, V. Berbenni, D. Capsoni, R. Riccardi, E. Antolini and B. Passalacqua, 1991. On the thermal stability and defect structure of the solid solution $\text{Li}_x\text{Ni}_{1-x}\text{O}$. *Solid State Ionics*, 45: 143-155.
- Nishida, Y., K. Nakane and T. Stoh, 1997. Synthesis and properties of gallium-doped LiNiO_2 as the cathode material for lithium secondary batteries. *J. Power Sources*, 68: 561-564.
- Ohzuku, T., A. Ueda and M. Nagayana, 1993. Electrochemistry and structural chemistry of LiNiO_2 (Rm) for 4 volt secondary lithium cells. *J. Electrochem. Soc.*, 140: 1862-1869.
- Ozawa, K., 1994. Lithium-ion rechargeable batteries with LiCoO_2 and carbon electrodes: the LiCoO_2/C system. *Solid State Ionics*, 69: 212-221.
- Peng, Z.S., C.R. Wan and C.Y. Jiang, 1998. Synthesis by sol-gel process and characterization of LiCoO_2 cathode materials. *J. Power Sources*, 72: 215-220.
- Shinova, E., E. Zhecheva, R. Stoyanova, G.D. Bromiley, R. Alcantara and J.L. Tirado, 2005. High-pressure synthesis and electrochemical behavior of layered $(1-a)\text{LiNi}_{1-y}\text{Al}_y\text{O}_2$ $a\text{Li}[\text{Li}_{1/3}\text{Ni}_{2/3}]\text{O}_2$ oxides. *J. Solid State Chem.*, 178: 2692-2700
- Song, M.Y. and D.S. Ahn, 1998. Improvement in the cycling performance of LiMn_2O_4 by the substitution of Fe for Mn. *Solid State Ion.*, 112: 245-248.
- Tarascon, J.M., E. Wang, F.K. Shokoohi, W.R. McKinnon and S. Colson, 1991. The spinel phase of LiMn_2O_4 as a cathode in secondary lithium cells. *J. Electrochem. Soc.*, 138: 2859-2863.
- Zhang, L., X. Wang, H. Noguchi, M. Yoshio, K. Takada and T. Sasaki, 2004. Electrochemical and *ex situ* XRD investigations on $(1-x)\text{LiNiO}_2 \cdot x\text{Li}_2\text{TiO}_3$ ($0.05 \leq x \leq 0.5$). *Electrochimica Acta*, 49: 3305-3311.